Matter-positronium interaction: An exact diagonalization study of the He atom - positronium system

A. Zubiaga,[*] F. Tuomisto, and M. J. Puska

Department of Applied Physics, Aalto University,

P.O. Box 11100, FIN-00076 Aalto Espoo, Finland

Abstract

The many-body system comprising a He nucleus, three electrons, and a positron has been studied using the exact diagonalization technique. The purpose has been to clarify to which extent the system can be considered as a distinguishable positronium (Ps) atom interacting with a He atom and, thereby, to pave the way to a practical atomistic modeling of Ps states and annihilation in matter. The maximum value of the distance between the positron and the nucleus is constrained and the Ps atom at different distances from the nucleus is identified from the electron and positron densities, as well as from the electron-positron distance and center-of-mass distributions. The polarization of the Ps atom increases as its distance from the nucleus decreases. A depletion of the He electron density, particularly large at low density values, has been observed. The ortho-Ps pick-off annihilation rate calculated as the overlap of the positron and the free He electron densities has to be corrected for the observed depletion, specially at large pores/voids.

---

[*] asier.zubiaga@aalto.fi

I. INTRODUCTION

The o-Ps atom is the bound state of an electron and a positron with total spin $S = 1$. In vacuum o-Ps has a relatively long lifetime of 142 ns because its annihilation via the fast two-gamma channel is prohibited by the conservation of the angular momemtum. Annihilation through the two-gamma channel with an electron of the matter having an opposite spin is possible when o-Ps interacts with matter. The resulting pick-off annihilation depends on the overlap of the o-Ps with the electron density of the matter and it can reduce the positron lifetime remarkably [1]. In metals and semiconductors the electron density is enhanced around the positron due to the attractive electron-positron interaction. This means that a Ps-like quasiparticle is created by the short-range screening of the positron by the electron cloud. In molecular matter and in some insulators such as SiO_2, the electron density is low in the interstitial regions and a Ps atom can be formed [2]. In this case the electron accompanying the positron hinders efficiently further screening of the positron by electrons in the matter. On the other hand, there is a finite overlap between the positron and the electrons of the material manifesting itself as the repulsive Pauli interaction and as the pick-off annihilation of o-Ps.

The pick-off annihilation lifetime spectroscopy of orto-Positronium (o-Ps) has a rather unique role as a method capable to study open volumes in soft or porous materials in which Ps is formed. Size and density distributions of nanometre-scale voids in polymers [3], porous SiO_2 [4, 5], and biostructures [6, 7] have been estimated by measuring the pick-off annihilation rate of o-Ps. However, in order to make a reliable quantitative analysis of the experimental results, one should be able to model o-Ps states and annihilation in these structures with predictive power.

In contrast to an atom where the nuclear degrees of freedom can, to a good approximation, be treated classically, both the electron and the positron in the Ps atom are light quantum-mechanical particles and the non-adiabatic correlation effects have to be taken into account. For positrons in dense materials, such as metals and semiconductors, a good starting point is a separate calculation of the quantum-mechanical state of a single positron [8]. In practice, this calculation is based on the results of many-body theories for a delocalized positron in a homogeneous electron gas. The nature of the Ps atom would call for a quantum-mechanical many-body calculation of the interacting electron-positron system in the Coulomb field of

nuclei. In the case of materials systems, this is clearly beyond the present computer capacity. An attractive starting point for modeling Ps is to consider it as a distinguishable particle also when it is interacting closely with matter. This is in line with the view of a long-living o-Ps interacting with matter and annihilating through a pick-off process.

The above-mentioned model of the Ps atom interacting as a single particle with matter finds support also from experimental and theoretical studies of Ps scattering off atoms and light molecules. Recently, the scattering of Ps off noble gas atoms and light molecules has been measured using a slow mono-energetic Ps beam [9]. The scattering properties of Ps have been seen to be dominated by the repulsive electron-electron Pauli interaction at short distances. At long distances the van der Waals attraction may play a role, especially in interactions with molecules of high polarizability.

The positronium Hydride (HPs) bound state has been observed experimentally by Schader et al. [10] and its binding energy has been estimated to be around 1.1 eV (0.04 Ha). The bound states of Ps with several small atoms have been studied theoretically using Exact Diagonalization techniques. The most carefully studied system is HPs [11–13], which has been found to form a bound state with a binding energy of 0.039 Ha, in good agreement with the experimental value. LiPs [11, 14, 15] and NaPs [11, 15] systems have also been predicted to form bound states with binding energies of 0.0123 Ha and 0.0084 Ha, respectively. The calculations show that at large distances the positron overlaps with an extra electron forming a free Ps-like cluster, while, when the positron density overlaps with that of the electrons inside the atom the Ps-like character is lost. In the case of closed-shell noble gas atoms the strong electron-electron Pauli repulsion dominates the atom-Ps interaction and the formation of bound states is prevented. Thus far, only a small number of different atoms have been considered in this kind of accurate calculations. However, it is already clear that the atoms able to trap Ps have high electron affinities and open-shell electronic structures [16].

Mitroy and Ivanov have studied the scattering of o-Ps off rare-gas atoms and alkali metal ions. [17, 18] They determined the scattering lengths for wave vectors up to 0.5 a_0^{-1} corresponding to the Ps energy of ~1.7 eV. Besides rare-gas atoms, also molecules have small electron affinities. They typically have HOMO-LUMO gaps of up to 1 Ha and their electrons are well localized in molecular orbitals. In polymers and biomolecular materials, the main cohesive interaction between the molecules is the van der Waals interaction and

their molecular orbitals are not greatly affected. Individual molecules still show HOMO-LUMO gaps and the repulsive Pauli interaction between electrons in neighboring molecules plays a role. On the other hand, the van der Waals interaction between the molecules and Ps can also be strong, especially for molecules of high polarizability.

A model widely used to study Ps in small pores and voids (< 2 nm) is that developed by Tao and Eldrup [19, 20]. The semi-empirical model relates the Ps lifetime and the pore/void radius. Ps is considered as a single particle and the pore/void is modeled using a spherical, cubic or elliptic infinite potential well. The electron density of the material enters the void and forms a layer of the thickness ΔR on its surface. The pick-off annihilation rate is calculated from the overlap of the positron density with the electron density of the material. The parameter of the model, ΔR, is not well known for all the materials and its chemical dependence cannot be described. In addition, the model assumes compact pores inside the material. The model has been extended to larger pores including the annihilation with excited particle-in-a-box states distributed according the Boltzmann distribution at a finite temperature. [21]

Schmitz and Müller-Plathe [22] introduced an atomistic model to describe Ps states and annihilation at voids in polymers. The potential landscape for Ps is based on the superposition of interactions between the Ps atom and individual atoms. These interactions, in turn, include the long-range van der Waals interaction based on the polarizabilities of the Ps atom and the atoms in the polymer and the short-range Pauli repulsion between the electron in the Ps atom and the electrons of the material. The latter interaction is described by fitting to experimental scattering cross sections. The Ps wave function corresponding to a given finite temperature is solved for by the path integral Monte-Carlo method and thereafter the pick-off annihilation rate is calculated as the overlap of the positron density with the electron density which is also obtained as a superposition over the atoms.

Our final goal is the atomistic modeling of a Ps atom interacting with molecular materials so that the necessary approximations made and the model parameters chosen are based on ab-initio results. Studying theoretically the HePs system will help to understand several aspects in the properties of Ps also in molecular solids and liquids. This is because in molecules electrons are also in a closed shell configuration and a HOMO-LUMO gap sets the minimum energy necessary for an extra electron (of the Ps atom) to enter into the electron cloud of the molecule.

The similarities between molecules with HOMO-LUMO gaps and closed-shell rare gas atoms in mind, we have calculated the many-body wavefunction and the total energy of the unbound HePs system by the exact diagonalization technique using a explicitly correlated Gaussians basis optimized by a stochastic variational method (ECG-SVM). In order to study the interaction of a Ps and a He atom at finite distances, the mean distance of the positron from the nucleus has been constrained. As a result, a set of configurations has been considered with the nucleus-positron mean distance ranging between 1.87 a_0 and 91.90 a_0. Electron and positron densities, interaction energies and annihilation rates have been calculated and analysed in order to clarify to which extent the picture of the distinguisable Ps particle can be applied.

II. STOCHASTIC VARIATIONAL METHOD AND THE MODELING OF THE HePs SYSTEM

We have described the N-particle system comprising the heavy nucleus (treated as a single particle), light electrons and the positron by the non-relativistic Hamiltonian

$$\widehat{H} = \sum_i \frac{\vec{p}_i^2}{2m_i} - T_{cm} + \sum_{i<j} \frac{q_i q_j}{4\pi\epsilon_0 r_{ij}}, \tag{1}$$

where $\vec{p}_i$, m_i, and q_i, are the momenta, masses, and charges of the particles, respectively, r_{ij} is the distance between the ith and j^{th} particles, and T_{cm} is the center-of-mass (CM) kinetic energy. The wavefunction is written as a linear combination of properly antisymmetrized explicitly correlated Gaussian (ECG) [23] functions as

$$\Psi = \sum_{i=1}^s c_i \, \psi_{SMs}^i(\vec{x}, A^i) = \sum_{i=1}^s c_i \, \mathcal{A} \left\{ \exp\left(-\tfrac{1}{2} \sum_{\mu,\nu=1}^{N-1} A_{\mu\nu}^i \vec{x}_\mu \vec{x}_\nu\right) \otimes \chi_{SMs} \right\}, \tag{2}$$

where $\mathcal{A}$ is an antisymmetrization operator and χ_{SMs} is the spin eigenfunction with $\hat{S}^2 \chi_{SMs} = S(S+1)\hbar^2 \chi_{SMs}$ and $\hat{S}_z \chi_{SMs} = M_S \hbar \chi_{SMs}$. We have considered only the spherically symmetric total angular momentum $L = 0$ states. The mixing coefficients c_i are obtained by diagonalizing the Hamiltonian matrix $< \psi_{SMs}^i |\widehat{H}| \psi_{SMs}^j >$. The nonlinear coefficients $A_{\mu\nu}^i$ are randomly generated and a new $A_{\mu\nu}^i$ is kept only if the update lowers the total energy of the system. Using the Jacobi coordinate set $\{\vec{x}_1,...,\vec{x}_{N-1}\}$, with the reduced mass of the ith coordinate as $\mu_i = m_{i+1} \frac{\sum_{i=1}^i m_i}{\sum_{i=1}^{i+1} m_i}$, allows for a straightforward separation of the

CM movement and therefore the total number of "particles" (degrees of freedom) treated is $N-1$.

The stochastic variational method (SVM) is suitable for calculating many-body wavefunctions, such as Ψ in Eq. (2), for small systems. [23] The number of particles is limited by the present algorithms and computer capacity typically to less than seven particles. The ECG basis comprises in our calculations 600 functions. The matrix elements between the basis functions are computed analytically in an efficient manner. In order to keep the size of the ECG basis small, the basis set is optimized by choosing the most appropriate non-linear parameters $A_{\mu\nu}^i$ for the Gaussian functions using a stochastic search in the parameter space. The large number of parameters to optimize, up to tens of thousands, prevents the use of direct search methods. The best non-linear parameter for each pair is chosen after 25 trials within each optimization cycle and 20 optimization cycles are done for each basis function. The trial values are obtained choosing values between a certain minimum and maximum using a random number generator.

SVM can be also used to study unbound systems setting boundaries to the possible values of the non-linear parameters $A_{\mu\nu}^i$, i. e. increasing the minimum value the particles can be prevented to separate to the infinity [17]. The configurations with the lowest energy are searched for within the available parameter space, i.e., the energy is minimized within a constrained parameter space. In order to model the interaction between He and the Ps atom at different distances it is enough to set a constraint only to the non-linear parameter $A_{\mu\nu}^i$ corresponding to the nucleus-positron pair. Thus, the size of the parameter space available for optimizing the wavefunction is not seriously restricted. The nucleus-positron distance parameter l_{He-p} corresponding to the maximum of the non-linear parameter, $A_{He-p}^i = (1/l_{He-p}^i)^2$, is varied between 1 and 50 a_0. The wavefunction and the total energy of the HePs system are then calculated for each constrained He-Ps distance. Due to practical reasons, the nucleus-electron distance parameter l_{He-e} also has to be limited. We have checked that using $l_{He-e}^i = 200$ a_0 gives structures and energies well-enough converged for our discussion below.

The kinetic energy ($\langle T \rangle$) and the potential energy ($\langle V \rangle$) of a system interacting through Coulomb potentials are related by the Virial theorem $2\langle T \rangle = -\langle V \rangle$. Any deviation from this relation is due to an inadequate basis function set. Optimizing the basis set the virial coefficient ($\frac{2\langle T \rangle}{\langle V \rangle} + 1$) decreases in magnitude.

In order to study the many-body wavefunction of the system, the positron ($\rho_p(r) = \langle \Psi | \delta(\vec{r}_p - \vec{r}_N - \vec{r}) | \Psi \rangle$) and electron ($\rho_e(r) = \sum_{i=1}^{N_e} \langle \Psi | \delta(\vec{r}_{i,e} - \vec{r}_N - \vec{r}) | \Psi \rangle$) density distributions are plotted. Above, $\vec{r}_N$ is the position vector of the nucleus and the index i runs over all the electrons N_e. The e-p pair correlation function is calculated as

$$\rho_{e-p}(\vec{r}) = \sum_{i=1}^{N_e} \langle \Psi | \delta(\vec{r}_i - \vec{r}_p - \vec{r}) | \Psi \rangle \tag{3}$$

The distribution of the electron-positron (e-p) CM is defined as

$$\rho_{ep}^{CM}(\vec{r}) = \sum_{i=1}^{N_e} \langle \Psi | \delta(\vec{r}_i^{CM} - \vec{r}) | \Psi \rangle \tag{4}$$

where $\vec{r}_i^{CM} = (\vec{r}_{i,e} + \vec{r}_p)/2$ is the center of mass of the positron and the ith electron and i runs over all the N_e electrons in the HePs system. The calculated distributions do not have any angular dependency and the radial distributions are the solid-angle averaged distributions multiplied by the radius squared.

The two electrons of the He atom are prepared in the $S = 0$ state while the electron and the positron of the o-Ps are in the $S = 1$ state. The total spin angular momentum of the system is, then, $S = 1$. For the pick-off annihilation rate Γ^{po}, the $S = 0$ component of the i^{th}electron-positron pair is selected through the $\widehat{P}_{S=0}^{i-p}$ spin projector, i.e.,

$$\Gamma^{po} = 4\pi r_0^2 c \sum_{i=1}^{N_e} \langle \Psi | \delta(\vec{r}_i - \vec{r}_p) \widehat{P}_{S=0}^{i-p} | \Psi \rangle \tag{5}$$

where r_0 is the classical electron radius and c is the speed of light. The summation runs over all the N_e electrons.

III.   RESULTS & DISCUSSION

Before discussing the main topic of this work, the identification of the Ps atom within the HePs system, we will shortly consider the energetics of the HePs system. The interaction energy E_I of HePs is defined as the difference between the total energy of the interacting system and the sum of the energies E_{He} and E_{Ps} of the isolated He and Ps atoms, respectively, i.e., $E_I = E_{HePs} - E_{He} - E_{Ps}$. E_{Ps}=-0.24999999999 Ha and E_{He} = -2.903693749 Ha have been obtained from SVM calculations with a basis of 56 functions (virial coefficient = 3.0×10^{-11}) and 600 functions (virial coefficient = 1.8×10^{-10}), respectively. The interaction

energy is shown in figure 1 as a function of the nucleus-positron mean distance $\langle r_p \rangle$. E_I is positive and approaches zero for large $\langle r_p \rangle$ values. For $\langle r_p \rangle$ smaller than 2.5 a_0, E_I is larger than E_{Ps}. Our calculations do not show the formation of the bound He-e$^+$ system. He can bind a positron only when it is in the $S = 3$ state [24] and its energy is 0.4 Ha above the the highest energy we have considered for the HePs system. It should be noticed that, already at 5 a_0, the interaction energy is clearly above the energy of a thermalized Ps.

Figure 1. Total interaction energy and its kinetic and potential energy contributions as a function of $\langle r_p \rangle$. The horizontal dotted line denotes the energy above which the Ps atom is unstable against dissociation. The inset shows the log-log plot of the virial coefficient versus $\langle r_p \rangle$.

The error of the interaction energy ΔE has been estimated as the total energy decrease after an optimization loop of the function basis. For the optimization loop the best non-linear parameter has been chosen for each pair after 25 trials. This procedure has been repeated 20 times for each basis function. For the most confined systems, $\langle r_p \rangle = 2$ a_0, $\Delta E = 0.01$ Ha and the virial coefficient is ~ 0.1. The confinement method shrinks the parameter space available to optimize the basis. In addition, the many-body wavefunction has to include the strong correlations happening in confined systems. Accordingly, the convergence is slow and the virial coefficient is large. For $\langle r_p \rangle = 48$ a_0, the error and the virial coefficient decrease to $\Delta E = 2 \times 10^{-5}$ Ha and 7×10^{-5}, respectively.

Figure 1 also shows the decomposition of the interaction energy to the kinetic and poten-

tial energy contributions. They are defined similarly to the total interaction energy. E_{Kin} is the main contribution to the interaction energy at distances shorter than 10 a_0, mostly due to the confinement of Ps and its small mass. E_{Pot} is always positive and at very short distances (< 4 a_0) it grows very fast.

The calculated mean distances of electrons $\langle r_e \rangle$, the positron $\langle r_p \rangle$ and the electron-positron CM $\langle r_{e-p}^{CM} \rangle$ from the He nucleus are shown in Fig. 2 as a function of the nucleus-positron distance parameter l_{He-p} corresponding to the confinement of the system. The mean distances grow monotonously because HePs is ultimately unbound. The fact that $\langle r_e \rangle$ increases with $\langle r_p \rangle$ is an indication of the formation of Ps. At $l_{He-p} < 5$ a_0, $\langle r_e \rangle$ saturates to a value of 2 a_0 because the electron of Ps does not penetrate into the He core. On the average, it stays at ~ 4 a_0 from the nucleus (see figure 4). On the other hand, $\langle r_{e-p}^{CM} \rangle$ continues to decrease because the positron keeps being confined.
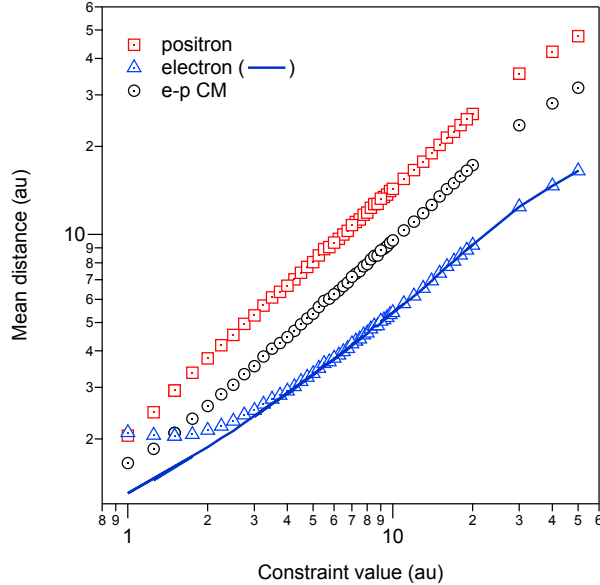

Figure 2. (Color online) Positron (red squares), electron (blue triangles) and electron-positron CM (black circles) mean distances from the He nucleus for different calculated configurations versus the nucleus-positron distance parameter l_{He-p}. The electron mean distance (blue line) obtained from the unpolarized Ps model is also given.

Using $\langle r_p \rangle$ and assuming that the Ps atom is not polarized, $\langle r_e \rangle$ can be approximated [25] as the sum of two thirds of the mean electron distance in the He atom of 0.93 a_0 and one third of the mean positron distance $\langle r_p \rangle$ (blue line in figure 2). The agreement with the $\langle r_e \rangle$

9

calculated from the many-body wavefunction is very good when $\langle r_p \rangle$ is larger than 7-8 a_0 (or the nucleus-positron distance parameter l_{He-p} is larger than 4-5 a_0). For smaller l_{He-p} values the actual $\langle r_e \rangle$ is larger than the estimated one which reflects the polarization of the Ps atom when approaching the He nucleus. The difference can actually be taken as a measure of the polarization (see figure 3). For $\langle r_p \rangle$=20 a_0 the polarization parameter is very small ($\sim 6 \times 10^{-3}$ a_0). The polarization starts to increase when $\langle r_p \rangle$ is below 10 a_0 and at 4 a_0 its value is $\sim$0.2 a_0 , i.e., 10% of the electron-positron mean distance for an isolated Ps. The maximum value of the polarization parameter is 0.8 a_0 when the interaction energy is 0.44 Ha and Ps is actually unstable against dissociation. According to our calculations, the smallest stable configuration corresponds to $\langle r_p \rangle \sim 2.9$ a_0 and a polarization parameter of $\sim$0.45 a_0.
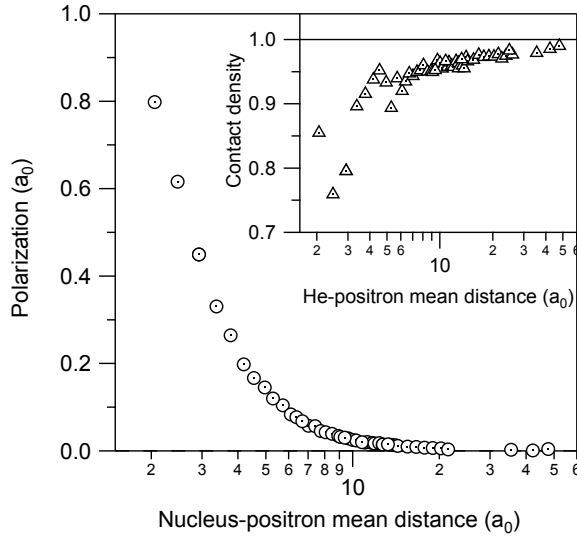

Figure 3. The polarization parameter for all the calculated HePs configurations as a function of the positron mean distance $\langle r_p \rangle$ from the He nucleus. The inset shows the electron-positron contact density corresponding to the Ps atom component as a function of $\langle r_p \rangle$. The solid line indicates the contact density of free Ps.

The electron-positron contact density of the Ps atom (shown in the inset of figure 3) has been obtained by subtracting the contribution of the He electrons estimated as two times the electron-positron contact density of the S=0 electron-positron pair. At $\langle r_p \rangle$=20 a_0, the contact density within the Ps atom reaches the value of 0.97, which is close to the exact

value of 1 for an isolated Ps. At $\langle r_p \rangle$=4 a_0 the contact density is still $\sim$0.94 and at the smallest separation decreases down to 0.76. The decrease of the contact density reflects and increasing polarization of the Ps atom in the interaction with the He atom.

Figure 4 shows the radial distributions of the positron and the electrons in HePs configurations corresponding to the positron mean distance $\langle r_p \rangle$ ranging from 3.4 a_0 to 13.7 a_0. The electron distribution can be decomposed into two components. The larger corresponds closely to the undisturbed electron density of a He atom. The second maximum overlaps with the positron distribution especially well for large $\langle r_p \rangle$ indicating the formation of a well-distinguishable Ps atom. At small separations, the overlap of the electron and positron distributions weakens, indicating the increase of the polarization of the Ps atom.
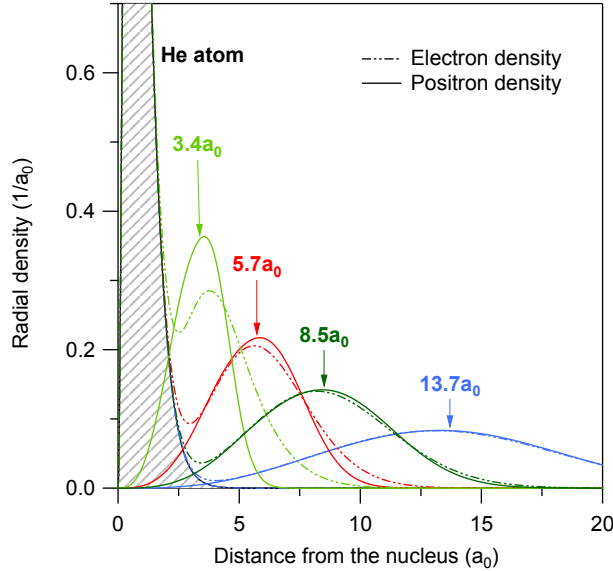

Figure 4. (Color online) Radial distributions of the positron (full lines) and electrons (dashed lines) for four different configurations of the HePs system with $\langle r_p \rangle$ values of 3.1 a_0 (light green), 5.2 a_0 (red), 7.5 a_0 (dark green) and 12.1 a_0 (blue). The arrowed tags indicate the position and the value of the positron mean distances $\langle r_p \rangle$ from the He nucleus for each configuration. The shading gives the electron density of a free He atom. All the distributions are normalized to the total number of particles.

Figure 5 shows the radial electron-positron correlation distribution for the four HePs configurations and for the isolated Ps atom. The distribution is calculated from equation (3) and it is normalized to the total number of electrons. When $\langle r_p \rangle = 3.4$ a_0, the electron-

positron pair correlation function shows a single peak but when $\langle r_p \rangle$ is above 5 a_0 a second peak starts to appear, as a shoulder, at 2 a_0. The shape and the magnitude of the second peak approach clearly to those for the isolated Ps atom and it corresponds to the electron-positron correlation inside the Ps atom. The second peak follows the positron distribution when it recedes from the He nucleus and it corresponds to the correlation between the positron and the electrons of the He atom. However, even at 8.5 a_0, the interaction between He and Ps affects the electron-positron correlations and the appearance of the Ps atom is not so clear-cut as in the electron distribution in figure 4.
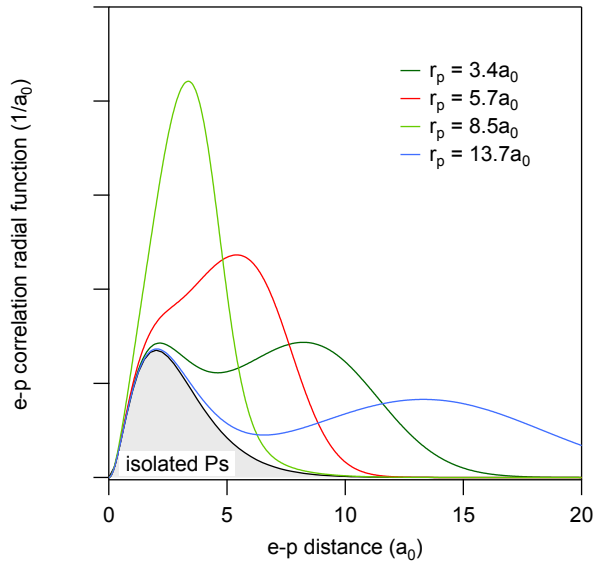

Figure 5. Electron-positron pair correlation function for the four HePs configurations of figure 4. The correlation distance for the isolated Ps atom (the dashed filled curve) is shown for comparison. All the electron-positron correlation curves are normalized to the number of electrons in the system in question.

The distribution of the e-p CM, shown in figure 6, can also be decomposed into two components. The larger component is closer to the He nucleus and its integrated intensity is double of that for the smaller and more delocalized component. Thus, the larger and the smaller components correspond to the two electrons of the He atom and the electron of the Ps atom, respectively. The Ps component is very similar to the positron radial density, especially when the mean He nucleus-positron distance is larger than 5 a_0.

Figure 7 shows the positron pick-off annihilation rate Γ^{po} as a function of $\langle r_p \rangle$, calculated
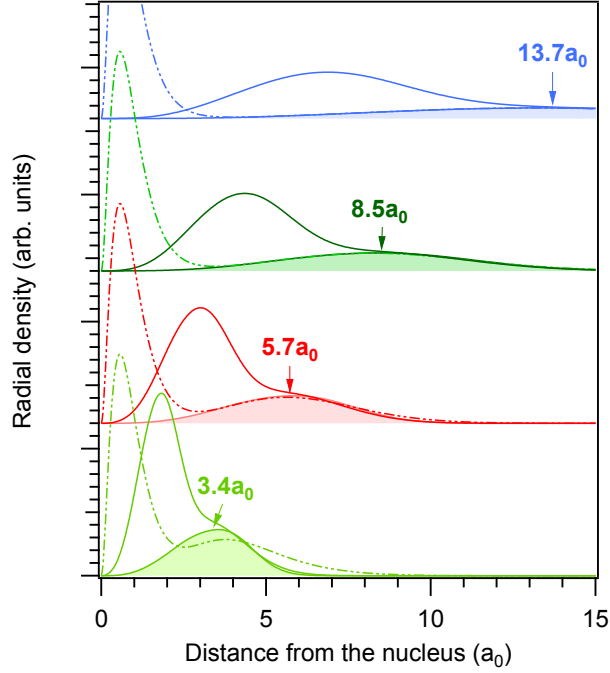
Figure 6. (Color online) Electron-positron CM distribution for the four HePs configurations. The electron (dashed) and the positron (filled areas) radial distributions are also shown for comparison. The CM distributions are normalized to the number of electrons.

using equation 5. It is an important magnitude for understanding Ps lifetime experiments in molecular matter and it also reflects the interaction of the Ps and He atoms and its behaviour. The projector $\widehat{P}_{S=0}^{i-p}$ in equation 5 ensures that the pick-off processes occur only with the He electron forming a spin-singlet state with the positron. Γ^{po} increases with the increasing overlap of the positron and He electron density. At $\langle r_p \rangle = 10$ a_0, Γ^{po} is about the same as the self-annihilation rate $\sim 7.04 \times 10^{-3}$ 1/ns of o-Ps (lifetime $\tau \sim 142$ ns). At 4 a_0, $\Gamma^{po} \sim 0.2$ 1/ns ($\tau \sim 4.8$ ns) and for $\langle r_p \rangle \sim 2.5$ a_0, Γ^{po} equals to 2 1/ns ($\tau = 500$ ps), the spin-averaged annihilation rate of Ps.

A non-selfconsistent positron pick-off annihilation rate is obtained from the overlap of the free He electron density $n_{e^-}^{He}$ and the SVM positron density n_{e^+} as

$$\Gamma_{ov}^{po} = 4\pi r_0^2 c \int d\vec{r} \, \frac{1}{2} n_{e^-}^{He}(\vec{r}) \, n_{e^+}(\vec{r}). \tag{6}$$

The free He electron density is from a SVM calculation and the factor one half reflects that only one electron in He annihilates with the positron. Γ_{ov}^{po} is widely used to calculate the pick-off annihilation rate of o-Ps [26]. With increasing nucleus-positron mean distance, it
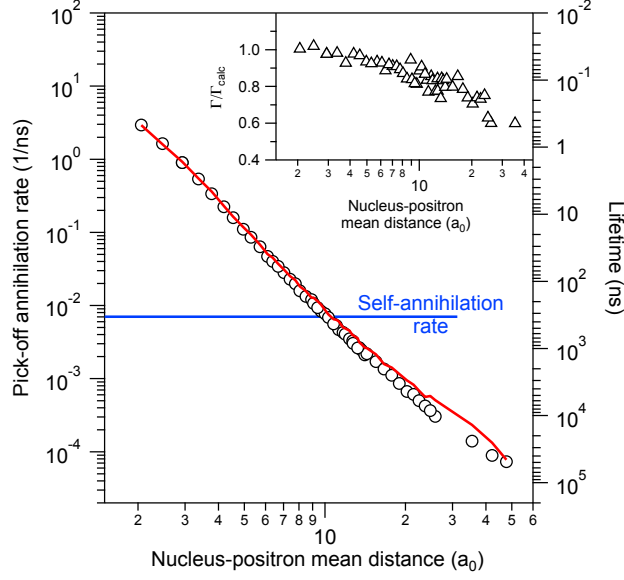
Figure 7. (Color online) Positron annihilation rate obtained from the SVM results using equation 5 (black circles) and from the overlap of the free He atom and the positron densities, using equation 6 (solid line). The inset show the ratio of the values. The blue horizontal line gives the self-annihilation rate of o-Ps.

agrees with the many-body Γ^{po} result until $\langle r_p \rangle \sim 5$ a_0 (solid line in figure 7). When $\langle r_p \rangle$ further increases, Γ^{po}_{ov} remains higher than Γ^{po}. The ratio $\Gamma^{po}/\Gamma^{po}_{ov}$, shown in the inset of figure 7, ranges between 1 and 0.6. The most confined systems show the largest ratios and it decreases steadily until $\langle r_p \rangle \sim 30$ a_0. At the level of the o-Ps self-annihilation rate the overlap of the annihilating positron with the He electrons has decreased by 20% compared to the undistorted He electron density. It should be noted that at large separations the overlap and the annihilation rate are very small, which is also reflected in the scatter of the overlap ratios. However, small values down to o-Ps self-annihilation rate are expected to be important for large voids.

In contrast to a positron in an electron gas, where the positron-electron contact density is enhanced [8], for Ps interacting with He the many-body effects induce a depletion of the contact density. The electron in Ps screens the charge of the positron and the electron-electron Pauli repulsion further decreases the contact density at the positron position, specially at low electron density values. Thus, in strongly confined systems the contact density is relatively weakly affected, but in weak confinement it is strongly depleted. Γ^{po}_{ov} needs to be

14

corrected for this effect specially when calculating the annihilation rate in large voids or pores, where the contact density is small and the annihilation rate is largely overestimated.

Figure 8 resumes the polarization parameter, He nucleus-positron mean distance and the interaction energy of the HePs system as a function of the positron lifetime $(1/\tau=\Gamma^{po}+1/142.05)$. The gray area marks where the interaction energy of Ps is larger than the Ps binding energy. The figure gives a clear idea about the magnitude of these quantities in different conditions.
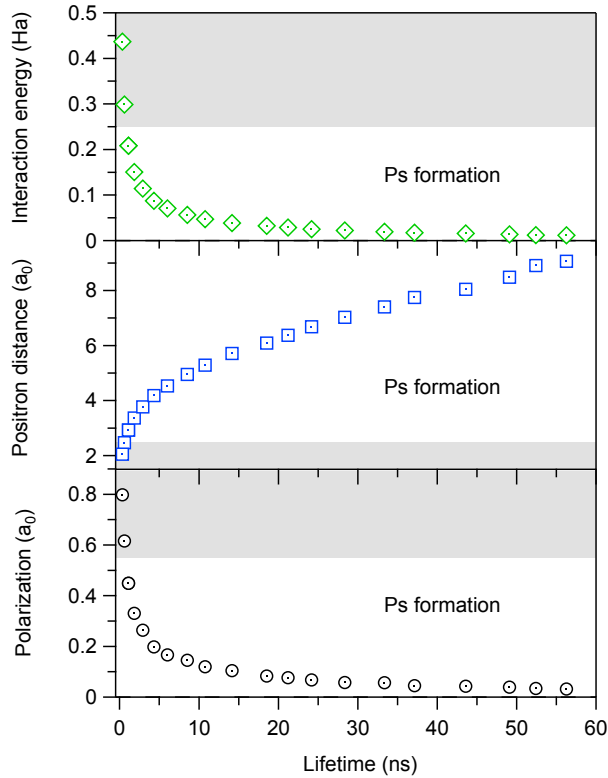

Figure 8. (Color online) The polarization (black circles), the He nucleus-positron distance (blue squares) and the interaction energy (green diamonds) of the HePs system as a function of the positron lifetime. The grey area indicates the value range where the interaction energy of Ps atom is larger than its binding energy.

IV. CONCLUSIONS

We have been interested in to what extent a separate Ps atom can be distinguished in a close interaction with a He atom, i.e., when the volume of the HePs system is constrained.

According to our many-body calculations the behavior of several measures, i.e., those of electron and positron mean distances from the He nucleus, electron and positron densities, as well as electron-positron pair correlation function and center-of-mass distribution show the formation of a Ps atom that is weakly polarized until the mean He nucleus-positron mean distance $\langle r_p \rangle$ is shorter than ~ 5 a_0. At shorter distances the Ps atom also forms but it is strongly polarized. The most clear-cut evidence is given, simply, by the electron and positron densities shown figure 4. There, the electron density can be decomposed into the He and Ps atom components and the positron density overlaps well with the electron density. Even at $\langle r_p \rangle \approx 5$ a_0 the positron-electron contact density is still high, ~ 93 % of that in the free Ps atom, and the polarization parameter indicating the imbalance of the electron and positron densities in the Ps atom is small, 0.2 a_0.

The above notions for the HePs system, generalized to molecules, supports the possibility to use a practical single-particle description for o-Ps in molecular materials. Many-body calculations could be used to define pairwise atom-Ps potentials which could form the basis for the calculation of the Ps energy landscape in the material and obtain, subsequently, its distribution and pick-off annihilation lifetime. In that respect, the above-mentioned findings about the relative depletion of the contact density, will simplify the reliable estimation of the pick-off annihilation rate.

[1] O. E. Mogensen, in *Positron Annihilation in Chemistry*, Vol. 58, edited by H. K. V. Lotsch (Springer-Verlag, 1995) Chap. Principles of Positron Annihilation in Molecular Solids, p. 193.

[2] S. V. Stepanov and V. M. Byakov, *Principles and application of positron & positronium chem-*

istry, edited by Y. C. Jean, P. E. Mallon, and D. M. Schrader, 5 (World Scientific, 2003) Chap. Physical and radiation Chemistry of the positron and positronium, p. 117.

[3] A. Uedono, R. Suzuki, T. Ohdaira, T. Uozumi, M. Ban, M. Kyoto, S. Tanigawa, and T. Mikado, J. Polym. Sci. Part B **36**, 2597 (1998).

[4] Y. Nagai, Y. Nagashima, and T. Hyodo, Phys. Rev. B **60**, 7677 (1999).

[5] L. Liszkay, C. Corbel, P. Perez, P. Desgardin, M.-F. Barthe, T. Ohdaira, R. Suzuki, P. Crivelli, U. Gendotti, A. Rubbia, M. Etienne, and A. Walcarius, Appl. Phys. Let. **92**, 063114 (2008).

[6] P. Sane, E. Salonen, E. Falck, J. Repakova, F. Tuomisto, J. Holopainen, and I. Vattulainen, J. Phys. Chem. B letters **113**, 1810 (2009).

[7] A. W. Dong, C. Pascual-Izarra, S. J. Pas, A. J. Hill, B. J. Boyd, and C. J. Drummond, J. Phys. Chem. B **113**, 84 (2009).

[8] M. J. Puska and R. M. Nieminen, Rev. Mod. Phys. **66**, 841 (1994).

[9] S. J. Brawley, S. Armitage, J. Beale, D. Leslie, A. Williams, and G. Laricchia, Science **330**, 789 (2010).

[10] D. M. Schrader, F. M. Jacobsen, N.-P. Frandsen, and U. Mikkelsen, Phys. Rev. Lett. **69**, 57 (1992).

[11] G. G. Ryzhikh, J. Mitroy, and K. Varga, J. Phys. B: At. Mol. Opt. Phys. **31**, 3965 (1998).

[12] J. Mitroy, Phys. Rev. A **73**, 054502 (2006).

[13] S. Bubin and K. Varga, Phys. Rev. A **84**, 012509 (2011).

[14] J. Mitroy, J. At. Mol. Sci. **1**, 275 (2010).

[15] J. Mitroy and G. G. Ryzhikh, J. Phys. B: At. Mol. Opt. Phys. **34**, 2001 (2001).

[16] J. Mitroy, M. W. J. Bromley, and G. G. Ryzhikh, J. Phys. B: At. Mol. Opt. Phys. **35**, R81 (2002).

[17] J. Mitroy and I. A. Ivanov, Phys. Rev. A **65**, 012509 (2001).

[18] J. Mitroy, J. Y. Zhang, and K. Varga, Phys. Rev. Lett. **101**, 123201 (2008).

[19] S. J. Tao, J. Chem. Phys. **56**, 5499 (1972).

[20] M. Eldrup, D. Lightbody, and J. N. Sherwood, Chem. Phys. **63**, 51 (1981).

[21] T. L. Dull, W. E. Frieze, D. W. Gidley, J. N. Sun, and A. F. Yee, J. Phys. Chem. B **105**, 4657 (2001).

[22] H. Schmitz and F. Müller-Plathe, J. Chem. Phys. **112**, 1040 (2000).

[23] K. Varga and Y. Suzuki, Phys. Rev. C **52**, 2885 (1995).

[24] J. Mitroy, Phys. Rev. A **72**, 032503 (2005).

[25] A. Zubiaga, F. Tuomisto, and M. Puska, "Study of unbound HePs using exact diagonalization technique," (2012), to be published in the Material Science Forum.

[26] W. Brandt, S. Berko, and W. W. Walker, Phys. Rev. **120**, 1289 (1960).